Published in final edited form as:
Stem Cells. 2014 April ; 32(4): 926–937. doi:10.1002/stem.1626.

Megakaryocytes contribute to the bone marrow-matrix environment by expressing fibronectin, type IV collagen and laminin

Alessandro Malara[1,2], **Manuela Currao**[1,2], **Cristian Gruppi**[1], **Giuseppe Celesti**[3], **Gianluca Viarengo**[4], **Chiara Buracchi**[5], **Luigi Laghi**[3], **David L. Kaplan**[6], and **Alessandra Balduini**[1,2,6]

[1]Department of Molecular Medicine, University of Pavia, Pavia, Italy

[2]Biotechnology Research Laboratories, IRCCS San Matteo Foundation, Pavia, Italy

[3]Laboratory of Molecular Gastroenterology, IRCCS Humanitas Clinical and Research Center, Rozzano, Milan, Italy

[4]Immunohaematology and Transfusion Service, Apheresis and Cell Therapy Unit, IRCCS San Matteo Foundation, Pavia, Italy

[5]Department of Immunology and Inflammation, IRCCS Humanitas Clinical and Research Center, Rozzano, Milan, Italy

[6]Department of Biomedical Engineering, Tufts University, Medford, MA, USA

Abstract

Megakaryocytes associate with the bone marrow vasculature where they convert their cytoplasm into proplatelets that protrude through the vascular endothelium into the lumen and release platelets. The extracellular matrix (ECM) microenvironment plays a critical role in regulating these processes. In this work we demonstrate that, among bone marrow ECM components, fibronectin, type IV collagen and laminin are the most abundant around bone marrow sinusoids and constitute a peri-cellular matrix surrounding megakaryocytes. Most importantly, we report, for the first time, that megakaryocytes express components of the basement membrane and that these molecules contribute to the regulation of megakaryocyte development and bone marrow ECM homeostasis both in vitro and in vivo. *In vitro*, fibronectin induced a three-fold increase in the proliferation rate of mouse hematopoietic stem cells leading to higher megakaryocyte output with respect to cells treated only with thrombopoietin or other matrices. However, megakaryocyte ploidy level in fibronectin-treated cultures was significantly reduced. Stimulation with type IV collagen resulted in a 1.4-fold increase in megakaryocyte output, while all tested matrices supported proplatelet formation to a similar extent in megakaryocytes derived from fetal liver progenitor cells. *In vivo*, megakaryocyte expression of fibronectin and basement membrane

Corresponding Author: Alessandra Balduini (alessandra.balduini@tufts.edu), Department of Biomedical Engineering, Tufts University, 4 Colby Street, Medford, MA 02155, USA. Biotechnology Research Laboratories, Department of Molecular Medicine, University of Pavia, IRCCS San Matteo Foundation, viale Forlanini 6, 27100 Pavia, Italy. Phone +39 0382 502984. Fax +39 0382 502990.

Authorship: AM, MC, CG, GC, GV, CB performed the research; AM and AB designed research, interpreted and analyzed the data; DK and LL analyzed data; AM and AB wrote the paper; AB provided overall direction.

Conflict of Interest: The authors declare no conflicts of interest.

components was up-regulated during bone marrow reconstitution upon 5-fluorouracil induced myelosuppression, while only type IV collagen resulted up-regulated upon induced thrombocytopenia. In conclusion, this work demonstrates that ECM components impact megakaryocyte behavior differently during their differentiation and highlights a new role for megakaryocyte as ECM-producing cells for the establishment of cell niches during bone marrow regeneration.

Keywords

Bone Marrow; Extracellular Matrix; Megakaryocyte; Myelosuppression

Introduction

The bone marrow (BM) microenvironment consists of various types of cells and their secreted extracellular matrix (ECM) components in a meshwork of capillary-venous sinouses, and plays a key role in the regulation of hematopoiesis. In general, ECM components interact with each other to form a structural framework that supports tissue organization and positional cues that regulate cellular processes. The importance of ECM components in the maintenance of correct hematopoiesis is clear as demonstrated by the alteration of this process observed in tenascin [1] and collagen type X knock-out mice [2].

Megakaryocytes (Mks) are rare cells in the bone marrow and, besides platelet release, growing evidences attribute new functions to these cells in the generation and maintenance of the bone marrow cell niche. Mks have been shown to be implicated in the regulation of osteoblast and osteoclast differentiation both *in vitro* and *in vivo* [3, 4, 5] and in the support of long-lived plasma cell niche in the bone marrow [6]. Further, Mks are the main source of pro- and anti-angiogenic proteins (Vascular Endothelial Growth Factor (VEGF), Thrombospondin-1 and Endostatin) [7] and the “fibrogenic” protein Transforming Growth Factor-β (TGF-β) involved in the onset of myeloproliferative disorders [8, 9]. Interestingly, Mks have been recently shown to be involved in matrix deposition and remodeling, as demonstrated by their role in fibronectin (FNC) fibrillogenesis [10] and the expression of matrix cross-linking enzymes, such as lysil oxidase [11] and factor XIIIa [10], essential in the dynamic of Mk-matrix component interactions.

The structure of niche microenvironment has been partly deciphered [12, 13]. Specifically, a monolayer of immature osteoblasts lines the bone defining the endostium, wherein hematopoietic stem cells (HSCs) reside. Many small vessels and sinusoids, in which trans-endothelial migration is thought to take place, are composed of specialized cell structures that regulate cell trafficking and constitute the vascular niche [14, 15]. In this scenario, Mks are supposed to differentiate from HSCs and to migrate in the direction of sinusoids, in the vascular “niche”, where platelets are released into bloodstream through the extension of long cytoplasmic protrusions called proplatelets [16, 17, 18]. Interestingly, individual ECM components were demonstrated to play a role in the regulation of Mk development *in vitro* [19, 20]. Fibronectin was shown to regulate Mk maturation [21] and proplatelet extension [22, 23, 24], while type III and type IV collagens were demonstrated to support proplatelet

formation *in vitro* [20]. In contrast, type I collagen is an important physiological inhibitor of platelet release *in vitro* [20, 25, 26, 27]. However, due to protection by bones, the BM remains one of the most difficult organs to study and data on its structural composition have mainly arisen from *in vitro* long term cultures of BM-derived cells [28, 29] and from immunofluorescence microscopy analysis [30, 31, 32].

In this paper we performed a systematic analysis of BM ECM composition along with spatial organization of single ECM components in mouse BM specimens. Further, we assessed the expression of different ECMs with particular attention to basement membrane components during murine megakaryopoiesis and tested their effects on HSC differentiation and Mk function *in vitro*. Finally, we showed that a distinct and specific increase in Mk derived ECM expression was determined by the administration of 5-fluorouracil or anti GPIbα antibody *in vivo*.

Methods

Animals

C57/BL6 mice were from Charles River Laboratories, Italy. Mice were housed at the animal facility of the Department of Physiology, section of General Physiology, University of Pavia (approval #1/2010, 24/06/2010). All animals were sacrificed according to the current European legal Animal Practice requirements.

Antibodies

Primary antibodies and dilutions are listed in Supporting Information Table1. 488 and 594 Alexa-conjugated secondary antibodies were purchased from Invitrogen (Milan, Italy, www.invitrogen.com).

Tissue collection, immunofluorescence and confocal microscopy

Femurs were removed from six to eight week old mice, fixed for 24 hours in paraformaldheyde (PFA) 3% and decalcified in a solution of EDTA 10%, in phosphate-buffered saline (w/o calcium and magnesium) (PBS) pH 7.2, for 2 weeks at 4°C. Specimens were embedded in Optical coherence tomography (OCT) cryosectioning medium, and snap frozen in a chilling bath. Eight μm-tissue sections were prepared by using a Microm Microtome HM 250 (Bio Optica S.p.A, Milan, Italy, www.bio-optica.it). For immunofluorescence staining sections were fixed for 20 minutes in 4% PFA, or alternatively with acetone at -20°C, washed with PBS, and blocked with 2% bovine serum albumin (BSA) (Sigma-Aldrich, Milan, Italy, www.sigmaaldrich.com) in PBS for 30 minutes. Nonspecific binding sites were saturated with a solution of 5% goat serum, 2% BSA and 0.1% glycine in PBS for 1 hour. Specimens were incubated with primary antibodies in washing buffer (0.2% BSA, 0.1% Tween 20 in PBS) overnight at 4°C. After three washes, sections were incubated with appropriate fluorescently-conjugated secondary antibodies in washing buffer for 1 hour at room temperature (RT). Nuclei were counterstained using Hoechst 33258 (100 ng/mL in PBS) at RT for 3 minutes. Sections were then mounted with micro-cover glass slips using Fluoro-mount (Bio-optica, Milan, Italy, www.bio-optica.it). Negative controls were routinely performed by omitting the primary antibodies (Supporting

Information Fig. S1C) while dot blot experiments were performed to exclude possible cross-reaction between antibodies and ECMs (Supporting Information Fig. S1B). Only a cross reaction of laminin antibody with nidogen was detected (Supporting Information Fig. S7). Details on immunohistochemistry protocol are detailed in Supporting Information.

All images were acquired using the Olympus BX51 fluorescence microscopy (Olympus Deutschland GmbH, Hamburg, Germany, www.olymbus-global.com) and 10X/0.30 or 20X/0.50 Oympus UplanF1 objectives. Confocal microscopy was performed by a TCS SP2 confocal laser scanning microscope (Leica, Heidelberg, Germany, www.leica.com) equipped with a 63× oil-immersion objective. Measurements of megakaryocyte diameters and distribution were performed with the Axiovision 4.5 software (Carl Zeiss, www.zeiss.com). At least one hundred randomly distributed whole Mks (CD41+ positive fragments were not considered) were measured from sections of three different mice. Spearman's rank correlation coefficients were calculated using GraphPad Prism 5.0 software (www.graphpad.com). Jasc Paint Shop Pro 8.0 software was used for the management of images and panels assembly.

Bone marrow and fetal liver cell purification and culture

BM cells were flushed from femurs and lineage negative cells purified with the lineage cell depletion kit (Miltenyi Biotech, Germany). Cells were cultured for 4 days in DMEM (Gibco, Milan, Italy) supplemented with 1% of penicillin/streptomycin, 1% of L-glutamine, 10% of fetal bovine serum (Gibco, Milan, Italy, www.invitrogen.com), and 10 ng/ml of recombinant mouse thrombopoietin (TPO) (Peprotech, UK, www.peprotech.com). Co-cultures with ECMs were performed seeding the cells with 10 μg of purified type I collagen from rat tail, laminin and type IV collagen from Engelbreth-Holm-Swarm mouse sarcoma (SantaCruz Biotechnologies Inc., www.scbt.com), while fibronectin was purified from human plasma [9]. In some experiments a particular condition called ECM-MIX was set by the addiction of 10 μg of type IV collagen, fibronectin and laminin in the ratio of 1:1:1 to mimic the ECM that surrounds Mks *in vivo*. ECMs were re-added every 24 hours until cells were collected for analysis. Fetal liver cells were isolated and cultured as previously described. Mks from BM and fetal liver cultures were purified using a 1.5/3% gradient of BSA or by immuno-magnetic separation using FITC anti-CD41 antibody and anti-FITC antibody coniugated to microbeads (Milteny Biotech, Italy, www.miltenyibiotech,com). A cell purity of 94±3% was estimated in flow cytometry as assessed by CD41 staining (Supporting Information Fig. S2B). Bone marrow lymphocytes and granulocytes/monocytes were stained with PE anti B220 and PE-Mac-1 antibodies and sorted from bone marrow mononuclear cells using anti PE immunomagnetic beads (Milteny Biotech, Italy, www.miltenyibiotech,com), according to manufacture instructions. Purity of isolated cells was analyzed by flow cytometry after PE-CY7 anti CD19 and FITC anti Gr-1 antibodies and estimated as 97,3±0,6 and 98,4±0,3, respectively (Supporting Information Fig.S2C).

Flow cytometry and megakaryocyte sorting

Analysis of cell viability was assessed by incubating cells with 5 μl of 7-AAD viability staining solution (Biolegend, Milan, Italy, www.biolegend.com). For hematopoietic stem cells identification, 2×10^5 lineage negative cells, cultured for 24 or 48 hours in the presence

of TPO and ECMs, were stained with FITC lineage cocktail, APC anti mouse Sca1 and PE anti-mouse CD117 antibodies for 30 minutes and identified as lineage negative/Sca-1+/CD117+ cells. Megakaryocytes at day 4 of culture were analyzed using APC anti mouse CD45, FITC anti mouse CD41 and PE anti mouse CD42b. Megakaryocyte output was calculated as the percentage of SSC ^{high}/FSC^{high}/CD45+/CD42+/CD41+ cells and normalized to the total number of CD45^{+} cells. For Mk ploidy, cells were fixed overnight in ice cold 70% ethanol at -20°C. Sample were incubated in PBS with 100 μg/ml of RNAse and propidium iodide solution and eventually stained with 5 μl of FITC anti mouse CD41. All samples were acquired with a Beckman Coulter Navios flow cytometer. Non-stained samples, FITC and PE-isotype controls were used to set the correct analytical gating. Off-line data analysis was performed using Beckman Coulter Navios software package. Cell sorting experiments were performed using a FACSAria IIu (3 lasers; BD Bioscience, www.bdbiosciences.com). Diva software (BD Pharmingen) was used for data acquisition and analysis. Megakaryocytes were sorted from bone marrow cells as CD41+/CD45+/cKit+/CD31+ population. Gate strategy is shown in Supporting Information Fig. S6.

RNA isolation and qualitative and quantitative polymerase chain reaction (PCR)

Detailed in Supporting Information

Platelet depletion and myelosuppression

Six to eight week old mice were given a sterile intra-peritoneal injection of anti–mouse GPIbα antibody (R-300, Emfret Analystics, www.emfret.com) (4μg/g of mouse) to induce an immune thrombocytopenia. Platelet and white blood cells counts were measured at 48, 72, 96, and 120 hours after injection. Myelosuppression was induced by 5-fluorouracil (5-FU) (250 mg/kg body weight, Sigma-Aldrich, Milan, Italy) injected intraperitoneally. At indicated time points, mice were sacrificed and blood collected for peripheral blood count. Femurs were fixed in PFA 3% or alternatively flushed and BM cells counted with trypan blue solution and then used for flow cytometry analysis. Age paired mice were injected with PBS as control.

Protein extraction and western blotting

Detailed in Supporting Information.

Statistics

Values are expressed as mean ± SD. Two tailed T-test and two way ANOVA were used to analyze experiments. A value of $p<0.05$ was considered statistically significant. All experiments were independently replicated at least three times.

Results

Megakaryocyte interaction with the endosteal and vascular “niches” in the bone marrow

Immunofluorescence analysis of Mk distribution demonstrated that these cells, although extremely rare, were present in the BM cavity at the diaphysis, metaphysis and epiphysis of femur sections as demonstrated by CD41 staining (Fig. 1A). Quantification of Mk density in

these districts, expressed as absolute number of Mks per mm^2 of marrow surface, demonstrated a slight increase in Mk concentration within the femur diaphysis (Fig, 1B). Diaphysis in mice shows peculiar features: absence of fat cells, bone trabeculae and a vascular cast comprised of small arterioles, veins and sinusoids. Thus, diaphysis was chosen as the site for further measurements to define the relationship between Mks, bone, arterioles and sinusoids within the BM. Osteopontin, α-SMA and VEGFR-3 were used as specific markers of these structures and analysis of CD41+ Mks distance from these BM elements demonstrated that Mks were closely associated with VEGFR-3+ sinusoids, with more than 90% of the Mks within 50 μm from a sinusoid (median 20,90) (n=168), while only ∼10% of cells were found within 50 μm from a α-SMA+ arteriole (median 65,46) (n=191) (Fig. 1C, D). In contrast, measurements for endostium-Mk interactions revealed that less than 5% of these cells were within 50 μm from bone sites (median 135,54) (n=252) (Fig. 1C, D).

To define the presence of a gradient of maturing Mks migrating from the endosteal “niche” to vascular compartments, the size of CD41+ Mks on femur sections was determined and correlated to Mk distance from the endostium (n=149) and the closest arteriole (n=126) or sinusoid (n=127). Results are reported as dot plots in Fig. 1E and demonstrated a significant correlation between Mk size and distance from sinusoids ($p<0.001$) and to a lesser extent from arterioles ($p<0.05$).

Localization of extracellular matrix proteins within bone marrow

Distributions of type I, III, IV, VI collagens, fibronectin, and laminin (containing β1 and γ1 chains) were mapped in BM by immunofluorescence. As demonstrated in Fig. 2A, bone structure composition comprised type I, type III collagens and fibronectin. Bone lining osteoblasts were also positive for type VI collagen staining. Negative staining in all bone structures resulted upon type IV collagen and laminin staining. Further, staining of different ECM components in the BM medullary cavity, demonstrated the presence of a network of matrices, which connected adjacent island of cells in the marrow. This network revealed a positive staining for fibronectin and type IV collagen, while only few fibers of type I and type III collagens were detected as confirmed by Masson's trichrome staining (Fig. S1A). BM vasculature is heterogeneously composed of arterioles, sinusoids and small capillaries. Staining of BM specimens demonstrated a distribution of type IV collagen, fibronectin and laminin in marrow sinusoids, while, type I, III and VI collagen deposition was mainly restricted to arterioles (Fig. 2A and Fig. S3).

Type IV collagen, laminin and fibronectin are components of the megakaryocyte environment *in vivo*

Analysis of matrix distribution in the marrow showed that maturing Mks were in tight contact with different ECM components in the medullary cavity. Co-localization studies and confocal microscopy analysis showed that Mks were surrounded by a peri-cellular matrix with a fibrillar structure that stained positive for type IV collagen, fibronectin and laminin (Fig. 2B, Suppl. Video 1,2,3). The presence of specific ECM components around maturing Mks *in vivo* allowed us to explore the possibility that those ECM components might be released by Mks themselves. To test this hypothesis lineage-negative cells from BM were further enriched in hematopoietic progenitors, through the selection of c-Kit+ cells, and

differentiated for 4 days in the presence of TPO into mature Mks. Analysis by RT and qRT-PCR of laminin, type IV collagen chains and fibronectin expression, demonstrated that progenitor cells and Mks expressed some of the laminin chains with a prevalence of the α5β1γ1 isoform (Laminin-10) (Fig. 3A) and type IV collagen α1α1α2 and α5α5α6 heterotrimers (Fig. 3B). Specifically, the expression of type IV collagen α5α5α6 heterotrimer characterized Mk development from lineage-/c-Kit+ progenitor cells (LK cells) (Fig. 3D). In contrast, fibronectin was expressed to a similar extent by both cell types, while integrin αIIb (CD41) expression was specific for Mks (Fig. 3C-D). Results from mRNA analysis were confirmed by western blotting of total cell lysates using polyclonal antibodies directed against laminin, type IV collagen and fibronectin (Fig. 3E). Analysis of purified proteins by coomassie blue staining demonstrated comparable molecular weights of bands with respect to bands detected in Mk lysate (Fig. S2A). Moreover, we analyzed the expression of different ECMs in other LKS derived lineages and demonstrated that the expression levels of ECMs were significantly increase in Mks with respect to B lymphocytes and CD11b (Mac-1) granulocytic/monocytic cells sorted from bone marrow mononuclear cells (Fig. 3F).

Impact of ECM on bone marrow progenitor cells development and Mk differentiation

To investigate the possible role of BM ECM components in regulating HSC differentiation into Mks, BM lineage negative progenitor cells were cultured with recombinant TPO, in the presence of individual ECM components. A combination of fibronectin, type IV collagen and laminin was used to mimic the Mk environment *in vivo* and called “ECM-MIX”. We found that the addition of 10 μg of purified fibronectin alone or in the ECM-MIX, induced a significant increase in cell viability after 24 and 48 hours of culture, as verified by flow cytometry after 7-AAD staining (*p value<0.05,**p value<0.01) (Fig. 4A). Further, fibronectin induced a rapid expansion of bone marrow progenitor cell number in culture. Specifically, analysis of hematopoietic stem cell proliferation demonstrated that TPO alone induced a three-fold increase in the number of lineage-/Sca1+/c-Kit+ (LSK) cells in 24 hours. Importantly, the addition of fibronectin (FNC), and not type I or IV collagens or laminin, to BM cells significantly increased these effects from 1.3%±0,17 LSK cells with TPO alone to 4.40%±1,21 LSK cells in TPO+FNC treated cells ($p<0.05$) (Fig. 4B, C). Finally, the number of LSK cells in the ECM-MIX condition showed a trend to increase, although not significant, with respect to TPO alone (Fig. 4B).

In the BM lineage-/c-kit+ fraction, only a small percentage of cells was positive for Mk markers at the beginning of the cultures, as revealed by CD41/CD42b staining in the CD45+ fraction by flow cytometry (Fig. 4D, **left panel**). However, after 72 hours of TPO stimulation in culture, BM lineage negative progenitor cells started to differentiate into Mks as revealed after CD41 staining with immunofluorescence (data not shown). The effects of ECM components on mouse megakaryopoesis were quantified after 96 hours of differentiation by flow cytometry (Fig. 4D, **right panel**). As shown in Fig. 4E, progenitor cells treated with TPO+FNC displayed a significant increase in the number of CD41+/CD42+/CD45+ Mks (3.52±0,8 relative to control, $p<0,001$). A slight increase in Mks was assessed also in type IV collagen (1.40±0,23, $p<0,05$) and laminin treated cells (1.19±0,3 p<n.s.). The results obtained in cells stimulated with the ECM-MIX combination showed

that the effects of fibronectin were reduced in the presence of other ECM components (1,81±0,1 relative to control, $p<0.05$). Interestingly, ploidy analysis revealed that Mks produced by bone marrow progenitor cells treated with fibronectin or ECM-MIX were more immature and resembled Mk progenitors as displayed by the increase in diploid/tetraploid cells and the reduction in mature 16N and 32N Mks (Fig. 4F). Moreover, to assess the effects of ECM components on proplatelet formation, the final step of Mk maturation, Mks differentiated from fetal liver progenitor cells were purified and challenged for 24 hours in adhesion to different ECM components. Quantification of proplatelet formation demonstrated that, with the exception of type I collagen, all the ECM components supported proplatelet formation, although, to different extents. Specifically, type IV collagen and laminin promoted proplatelet formation to a higher extent (Fig. 4G).

Megakaryocytes express ECM components that participate to bone marrow matrix environment regeneration

To determine the significance of ECM components synthesis by mouse Mks *in vivo*, we evaluated their expression during a state of "stressed hematopoiesis" after 5-FU induced myelosuppression or after platelet depletion by an anti GPIbα antibody. Both treatments determined a rapid decrease in peripheral platelet count (Fig. 5A). Recovery of peripheral platelets started after 10 days of 5-FU treatment and after 72 hours of anti GPIbα injection, respectively. Further, a marked decrease in peripheral leukocyte count and BM cellularity was found, and complete disruption of vasculature with areas of haemorrage was observed in 5-FU treated mice (Fig, 5B-C and G). Most importantly, an increase in BM Mk contents was observed in concomitance with platelet recovery in both treated mice with a more pronounced increase in 5-FU treated mice as shown by flow cytometry analysis (Fig. 5D-E) and BM sections staining (Fig. 5F-G). Interestingly, at day 10 of 5-FU Mks represented the major fraction of myeloid cells during marrow recovery as revealed by the prolonged delay in granulocyte and monocyte recovery (Fig. S5A-B and C), but not of the lymphoid compartment (Fig. S5D). In order to study the role of Mk derived ECMs in the regeneration of BM and platelet count, BM Mks were sorted at their peak of increase, at day 2.5 (anti GPIbα) and at day 10 (5-FU) after drug administration, and analyzed for ECM expression (Fig. 6A). Interestingly, we observed two different pattern of ECM up-regulation depending on the type of treatment. Specifically, in GPIbα treated mice only a significant increase of type IV collagen was observed in BM Mks at both mRNA and protein levels (Fig. 6B-D). In contrast, an important increase of laminin, type IV collagen and fibronectin was observed in BM Mks derived from 5-FU treated mice (Fig. 6C-E) coincidently with the restoration of general bone marrow ECM content (Fig. S4A-B).

Discussion

Mature Mks reside predominantly next to BM sinusoids, juxtaposed to vascular endothelial cells. This evidence has been derived from the observation of marrow biopsies [30, 31] and more recently from the analysis of the BM of living mice using *in vivo* intravascular two photon microscopy technique [32]. However, the connection between Mks and BM environment components is not completely understood. In this work, we first measured the distances of CD41+ Mks from specific structures of the endosteal and vascular "niches" in

murine BM [17, 33]. We found a significant correlation between Mk dimension and their distance from sinusoids, showing the presence of a gradient of maturing-Mks in the vascular niche. These data are in line with the necessity of mature Mks to extend long cytoplasmatic processes, called proplatelets, through the fenestrations of the endothelial cell layer and into the vascular space, where platelets are shed into the circulation [32]. Moreover, we mapped the localization of different collagens and glycoproteins that have been shown to be involved in the regulation of Mk differentiation or function *in vitro* [18, 19, 27]. These results confirm and extend previous analysis of the ECM component composition of mouse BM [28, 29] by demonstrating that, in the BM, Mks are surrounded by large fibrils that stain positive for fibronectin, and the basement membrane components type IV collagen and laminin. In order to decipher the origin of these ECM components, we analyzed their expression in Mks differentiated from BM progenitor cells. We previously demonstrated that human Mks express fibronectin [9] and that the genetic profile of Mks, differentiated human CD34+ HSCs, is characterized by an increase in the expression of nidogen [34]. Building on these data, in this work we showed that Mks also express laminin, with a prevalence of the isoform 10 (α5β1γ1), and type IV collagen heterotrimers (α1α1α2 and α5α5α6). Additionally, during Mk differentiation from myeloid progenitors cells (Lineage-/c-Kit+) we found, by RT-PCR, comparable levels of fibronectin and laminin 10 expression, while the expression of type IV collagen α5/α6 was a specific feature of mature Mks. Interestingly, the *in vivo* expression levels of these ECMs were significantly higher in Mks with respect to others LKS derived lineages, such as B cells and granulocytic/monocytic cells. Type IV collagen and laminin are abundant components of basement membranes that represent the thin layer of extracellular matrix that delineates endothelial/epithelial cells from adjacent stromal tissue. Basement membranes play pivotal roles in tissue development and maintenance, acting as adhesive substrates, binding growth factors and providing mechanical strength to tissues and organs [35, 36]. On this basis, our results demonstrated, for the first time, that mouse primary Mks express basement membrane components that may regulate their function in both physiological and pathological conditions. To test this possibility, bone marrow hematopoietic progenitor cells and differentiated Mks were challenged *in vitro* with purified preparation and combinations of ECMs. We found that only fibronectin was able to increase cell survival and proliferation on lineage negative BM cells. Specifically, we showed that fibronectin in combination with TPO significantly increased the number of lineage-/c-Kit+/Sca1+ cells, enlarging the pool of HSCs available for Mk maturation and development. However, these cells resembled Mk progenitors as demonstrated by a reduced maturational stage as highlighted by ploidy analysis. These results further support previous work where fibronectin was demonstrated to be important for Mk expansion from human hematopoietic progenitor cells [37] and its binding to its receptors (alpha4/beta1 and alpha5/beta1) a requirement for Mk development and maturation *in vitro* [20]. Importantly, type IV collagen exerted a different effect than fibronectin, increasing the number of Mks without affecting Mk maturational stage, while laminin promoted only a slight increase of Mk output. This observed effect of laminin maybe ascribed to the fact that the commercial purified laminin-1 was used in these experiments, although it is now known, that different laminin isoforms can serve distinct functions and the alpha5 subunit could exert a specific or peculiar effect on stem cells and Mk function [38]. Interestingly, the mixture of fibronectin, type IV collagen and laminin did

not enhance the effect of the single ECMs. This could be the result of ECM mutual interaction [39, 40] with the consequence of reduced levels of ECMs available for Mk binding and activation. Overall, these data may suggest that the interaction of different ECMs lead to modulation of their impact on Mk function. Finally, to define the physiological role of ECM production by murine Mks *in vivo*, we analyzed the behavior of their "ECM core" upon induced thrombocytopenia by anti GPIbα antibody treatment [41] or myelosuppression by 5-FU administration. Both these treatment led to an increase of the bone marrow Mk population that peaked after 10 and 3 days after drug administration respectively. Bone marrow Mk were sorted at their peak of proliferation for each treatment and analyzed for ECM expression. Interestingly, we observed a peculiar profile of ECM expression in Mks depending on the type of treatment. Specifically, Mk sorted from mice undergoing platelet depletion, showed minimal changes in expression profile of genes that regulates type IV collagen, laminin and fibronectin production. Only a significant increase at the protein level for type IV collagen production was detected. Further, expansion of Mk during platelet recovery was not accompanied by changes in ECM components distribution and contents. In contrast, the experiments demonstrated that on day 10 post-5-FU administration, Mks occupied most of the extra-vascular space within bone marrow, with other myeloid cells almost absent [42]. These events were accompanied by an increase in bone marrow content of ECM components and followed by peripheral platelets count recovery simultaneous with the regeneration of bone marrow vasculature as described by Kopp et al [43]. Interestingly, analysis of Mk-ECM content in sorted Mks at day 10 of 5-FU treatment displayed a significant increase in the expression of fibronectin and basement proteins at both molecular and protein levels. These data strengthened the hypothesis of Mks as ECM-producing cells and suggested the possible involvement of Mks in the establishment of the bone marrow-matrix environment. The exact signals that regulate ECM expression by Mks *in vivo* are still to be completely clarified. However, in support of these data, the contributions of Mks to the vascular niche have only recently emerged as demonstrated by the release of pro/anti angiogenic factors [7], ECM cross-linking enzymes [9, 10] or plasma cell survival factors such as interleukin-6 and proliferation-inducing ligand within BM [5].

Conclusions

In conclusion, we have deciphered the ECM composition of the Mk environment and demonstrated that these cells express basement membrane proteins in close proximity to sinusoidal endothelial cells. Importantly, we also showed that ECM components differently modulate HSC and Mk development *in vitro*, reflecting the importance of their spatial localization and cell interactions *in vivo*. Finally, we demonstrated that the production of endogenous ECM components is not related to the physiological production of platelets *in vivo* but significantly boosted concomitantly to the regeneration of bone marrow environment following myelosuppression. We believe that the mayor outcome of these discoveries could be a link to human diseases, such as myeloproliferative disorders, where altered megakaryopoyesis and myelofibrosis are distinctive features [44].

Supplementary Material

Refer to Web version on PubMed Central for supplementary material.

Acknowledgments

We thank Patrizia Vaghi (University of Pavia, Italy) for technical assistance with confocal microscopy analysis, Paolo Catarsi (San Matteo Foundation, Pavia, Italy) for technical assistance with qRT-PCR analysis, Alessandro Pecci (University of Pavia) for assistance with Axiovision 4.5 software, Cesare Balduini and Maria Enrica Tira (University of Pavia) for helpful discussion on the manuscript, Alfonso Colombatti (CRO, Aviano, Italy) for the anti nidogen antibody. This paper was supported by Cariplo Foundation (2010-0807), Regione Lombardia - Project SAL-45, Almamater Foundation (Pavia) and Regione Lombardia- Progetto di cooperazione scientifica e tecnologica internazionale, Associazione Italiana per la Ricerca sul Cancro (AIRC, Milano) “Special Program Molecular Clinical Oncology 5×1000” to AGIMM (AIRC-Gruppo Italiano Malattie Mieloproliferative), US National Institutes of Health (grant EB016041-01) and Italian Ministry of Health (grant RF-2009-1550218). The funders had no role in study design, data collection and analysis, decision to publish, or preparation of the manuscript.

References

1. Ohta M, Sakai T, Saga Y, et al. Suppression of hematopoietic activity in tenascin-C-deficient mice. Blood. 1998; 1:4074–83. [PubMed: 9596652]
2. Jacenko O, Roberts DW, Campbell MR, et al. Linking hematopoiesis to endochondral skeletogenesis through analysis of mice transgenic for collagen X. Am J Pathol. 2002; 160:2019–34. [PubMed: 12057907]
3. Kacena MA, Nelson T, Clough ME, et al. Megakaryocyte-mediated inhibition of osteoclast development. Bone. 2006; 39:991–9. [PubMed: 16782418]
4. Ciovacco WA, Cheng YH, Horowitz MC, Kacena MA. Immature and mature megakaryocytes enhance osteoblast proliferation and inhibit osteoclast formation. J Cell Biochem. 2010; 109:774–781. [PubMed: 20052670]
5. Winter O, Moser K, Mohr E, et al. Megakaryocytes constitute a functional component of a plasma cell niche in the bone marrow. Blood. 2010; 116:1867–75. [PubMed: 20538807]
6. Italiano JE Jr, Richardson JL, Patel-Hett S, et al. Angiogenesis is regulated by a novel mechanism: pro- and antiangiogenic proteins are organized into separate platelet alpha granules and differentially released. Blood. 2008; 111:1227–33. [PubMed: 17962514]
7. Ciurea SO, Merchant D, Mahmud N, et al. Pivotal contributions of megakaryocytes to the biology of idiopathic myelofibrosis. Blood. 2007; 110:986–93. [PubMed: 17473062]
8. Badalucco S, Di Buduo CA, Campanelli R, et al. Involvement of TGFβ1 in autocrine regulation of proplatelet formation in healthy subjects and patients with primary myelofibrosis. Haematologica. 2013; 98:514–7. [PubMed: 23403314]
9. Malara A, Gruppi C, Rebuzzini P, et al. Megakaryocyte-matrix interaction within bone marrow: new roles for fibronectin and factor XIII-A. Blood. 2011; 117:2476–83. [PubMed: 21131589]
10. Eliades A, Papadantonakis N, Bhupatiraju A, et al. Control of megakaryocyte expansion and bone marrow fibrosis by lysyl oxidase. J Biol Chem. 2011; 286:27630–8. [PubMed: 21665949]
11. Haylock DN, Nilsson SK. Stem cell regulation by the hematopoietic stem cell niche. Cell Cycle. 2005; 4:1353–5. [PubMed: 16123595]
12. Scadden DT. The stem-cell niche as an entity of action. Nature. 2006; 441:1075–9. [PubMed: 16810242]
13. Kaplan RN, Psaila B, Lyden D. Niche-to-Niche migration of bone marrow-derived cells. Trends in Molecular Medicine. 2007; 13:72–81. [PubMed: 17197241]
14. Yin T, Li L. The stem cell niches in bone. J Clin Invest. 2006; 116:1195–201. [PubMed: 16670760]
15. Avecilla ST, Hattori K, Heissig B, et al. Chemokine-mediated interaction of hematopoietic progenitors with the bone marrow vascular niche is required for thrombopoiesis. Nat Med. 2004; 10:64–71. [PubMed: 14702636]

16. Italiano JE Jr, Patel-Hett S, Hartwig JH. Mechanics of proplatelet elaboration. J Thromb Haemost. 2007; 5(Suppl1):18–23. [PubMed: 17635704]
17. Hooper AT, Butler JM, Nolan DJ, et al. Engraftment and reconstitution of hematopoiesis is dependent on VEGFR2-mediated regeneration of sinusoidal endothelial cells. Cell Stem Cell. 2009; 4:263–74. [PubMed: 19265665]
18. Larson MK, Watson SP. Regulation of proplatelet formation and platelet release by integrin alpha IIb beta3. Blood. 2006; 108:1509–14. [PubMed: 16670270]
19. Balduini A, Pallotta I, Malara A, et al. Adhesive receptors, extracellular proteins and myosin IIA orchestrate proplatelet formation by human megakaryocytes. J Thromb Haemost. 2008; 6:1900–7. [PubMed: 18752571]
20. Fox NE, Kaushansky K. Engagement of integrin alpha4beta1 enhances thrombopoietin-induced megakaryopoiesis. Exp Hematol. 2005; 33:94–9. [PubMed: 15661402]
21. Jiang F, Jia Y, Cohen I. Fibronectin- and protein kinase C-mediated activation of ERK/MAPK are essential for proplatelet-like formation. Blood. 2002; 99:3579–84. [PubMed: 11986211]
22. Matsunaga T, Fukai F, Kameda T, et al. Potentiated activation of VLA-4 and VLA-5 accelerates proplatelet-like formation. Ann Hematol. 2012; 91:1633–43. [PubMed: 22644786]
23. Chen Z, Naveiras O, Balduini A, et al. The May-Hegglin anomaly gene MYH9 is a negative regulator of platelet biogenesis modulated by the Rho-ROCK pathway. Blood. 2012; 110:171–9. [PubMed: 17392504]
24. Pallotta I, Lovett M, Rice W, et al. Bone marrow osteoblastic niche; a new model to study physiological regulation of megakaryopoiesis. Plos One. 2009; 4:e8359. [PubMed: 20027303]
25. Chang Y, Auradé F, Larbret F, et al. Proplatelet formation is regulated by the Rho/ROCK pathway. Blood. 2007; 109:4229–36. [PubMed: 17244674]
26. Lai Y, Sun Y, Skinner CM, et al. Reconstitution of marrow-derived extracellular matrix ex vivo: a robust culture system for expanding large-scale highly functional human mesenchymal stem cells. Stem Cells Dev. 2010; 19:1095–107. [PubMed: 19737070]
27. Celebi B, Mantovani D, Pineault N. Effects of extracellular matrix proteins on the growth of hematopoietic progenitor cells. Biomed Mater. 2011; 6:055011. [PubMed: 21931196]
28. Takaku T, Malide D, Chen J, et al. Hematopoiesis in 3 dimensions: human and murine bone marrow architecture visualized by confocal microscopy. Blood. 2010; 116:e41–55. [PubMed: 20647571]
29. Nilsson SK, Debatis ME, Dooner MS, et al. Immunofluorescence characterization of key extracellular matrix proteins in murine bone marrow in situ. J Histochem Cytochem. 1998; 46:371–7. [PubMed: 9487119]
30. Tavassoli M, Aoki M. Localization of megakaryocytes in the bone marrow. Blood Cells. 1989; 15:3–14. [PubMed: 2649185]
31. Tavassoli M, Aoki M. Migration of entire megakaryocytes through the marrow-blood barrier. Br J Haematol. 1981; 48:25–9. [PubMed: 7248188]
32. Junt T, Schulz H, Chen Z, et al. Dynamic visualization of thrombopoiesis within bone marrow. Science. 2007; 317:1767–70. [PubMed: 17885137]
33. Li XM, Hu Z, Jorgensen ML, Slayton WB. High levels of acetylated low-density lipoprotein uptake and low tyrosine kinase with immunoglobulin and epidermal growth factor homology domains-2 (Tie2) promoter activity distinguish sinusoids from other vessel types in murine bone marrow. Circulation. 2009; 120:1910–1918. [PubMed: 19858415]
34. Balduini A, d'Apolito M, Arcelli D, et al. Cord blood in vitro expanded CD41 cells: identification of novel components of megakaryocytopoiesis. J Thromb Haemost. 2006; 4:848–60. [PubMed: 16634756]
35. Sanes JR. The basement membrane/basal lamina of skeletal muscle. J Biol Chem. 2003; 278:12601–12604. [PubMed: 12556454]
36. Yurchenco PD, Amenta PS, Patton BL. Basement membrane assembly, stability and activities observed through a developmental lens. Matrix Biol. 2004; 22:521–538. [PubMed: 14996432]
37. Deutsch V, Hubel E, Kay S, et al. Mimicking the haematopoietic niche microenvironment provides a novel strategy for expansion of haematopoietic and megakaryocyte-progenitor cells from cord blood. Br J Haematol. 2010; 149:137–49. [PubMed: 20085580]

38. Gu YC, Kortesmaa J, Tryggvason K, et al. Laminin isoform-specific promotion of adhesion and migration of human bone marrow progenitor cells. Blood. 2003; 101:877–85. [PubMed: 12393739]

39. Shimizu M, Minakuchi K, Moon M, et al. Difference in interaction of fibronectin with type I collagen and type IV collagen. Biochim Biophys Acta. 1997; 1339:53–61. [PubMed: 9165099]

40. Rao CN, Margulies IM, Liotta LA. Binding domain for laminin on type IV collagen. Biochem Biophys Res Commun. 1985; 128:45–52. [PubMed: 3921025]

41. Dhanjal TS, Pendaries C, Ross EA, et al. A novel role for PECAM-1 in megakaryocytokinesis and recovery of platelet counts in thrombocytopenic mice. Blood. 2007; 109:4237–44. [PubMed: 17234740]

42. Radley JM, Scurfield G. Effects of 5-fluorouracil on mouse bone marrow. Br J Haematol. 1979; 43:341–51. [PubMed: 497116]

43. Kopp HG, Avecilla ST, Hooper AT, et al. Tie2 activation contributes to hemangiogenic regeneration after myelosuppression. Blood. 2005; 106:505–13. [PubMed: 15817675]

44. Papadantonakis N, Matsuura S, Ravid K. Megakaryocyte pathology and bone marrow fibrosis: the lysyl oxidase connection. Blood. 2012; 120:1774–81. [PubMed: 22767499]

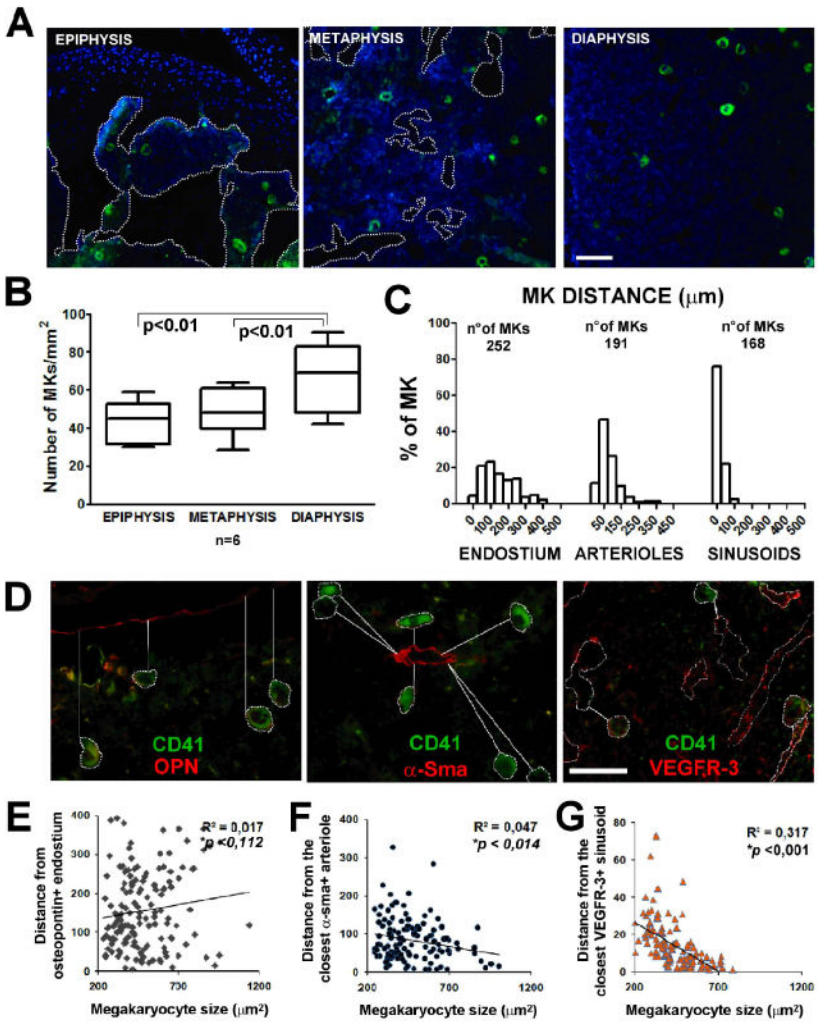

Figure 1.

Megakaryocyte localization within the bone marrow. **A**) Immunofluorescence staining of CD41+ Mks (green) in bone marrow of mouse femur. Images were acquired with a 10x/0.30 Olympus UPlanF1 objective. Scale Bar=100 μm. **B**) Quantification of Mks in epiphysis, metaphysis and diaphysis of mouse femur. Axiovision 4.5 software was used to perform this analysis expressed as absolute number of Mks per mm^2 of bone marrow surface. p value <0.01. **C**) Distribution of Mks related to their distance from osteopontin (OPN) positive endosteal surface, α-smooth muscle actin (α-SMA) positive arterioles and VEGFR-3 positive sinusoids within bone marrow. **D**) Immunofluorescence staining of CD41+ Mks (green) in proximity of OPN, α-SMA, VEGFR-3 positive structures (red). Images were acquired using 40x objective. Scale Bar=100 μm. All images were acquired using the Olympus BX51 fluorescence microscopy. **E-F-G**) Correlation between Mk dimension and distance from endosteal surface, arterioles and sinusoids. R, Spearman's correlation coefficient; line shows non linear regression; p, p value.

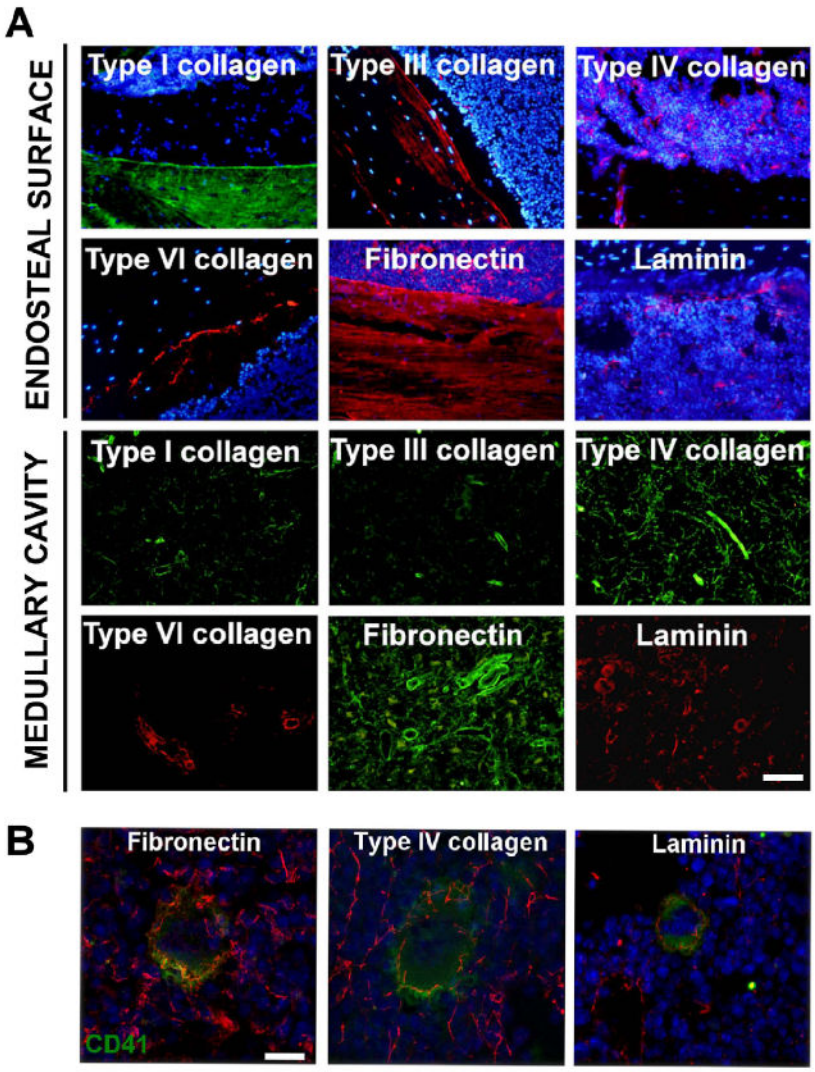

Figure 2.

Bone marrow extracellular matrix distribution at endosteal and vascular districts. **A**) Immunofluorescence analysis of ECM component distribution at endosteal surface and medullary cavity of mouse femur. Images in the endosteal "niche" were acquired at the interface between diaphyseal bone and bone marrow cells. A 20x/0.50 Olympus UPlanF1 objective was used. Scale Bar=100 μm. Hoechst 33258 was used to stain nuclei (blue). **B**) Confocal microscopy analysis of *ex vivo* Mk-ECM interaction within bone marrow demonstrated that Mk (CD41+, green) were surrounded by a peri-cellular matrix positive for fibronectin, type IV collagen and laminin (red). Confocal microscopy was performed by a TCS SP2 confocal laser scanning microscope (Leica, Heidelberg, Germany) equipped with a 63× oil-immersion objective. Scale bar=20 μm. Hoechst 33258 was used to stain nuclei (blue).

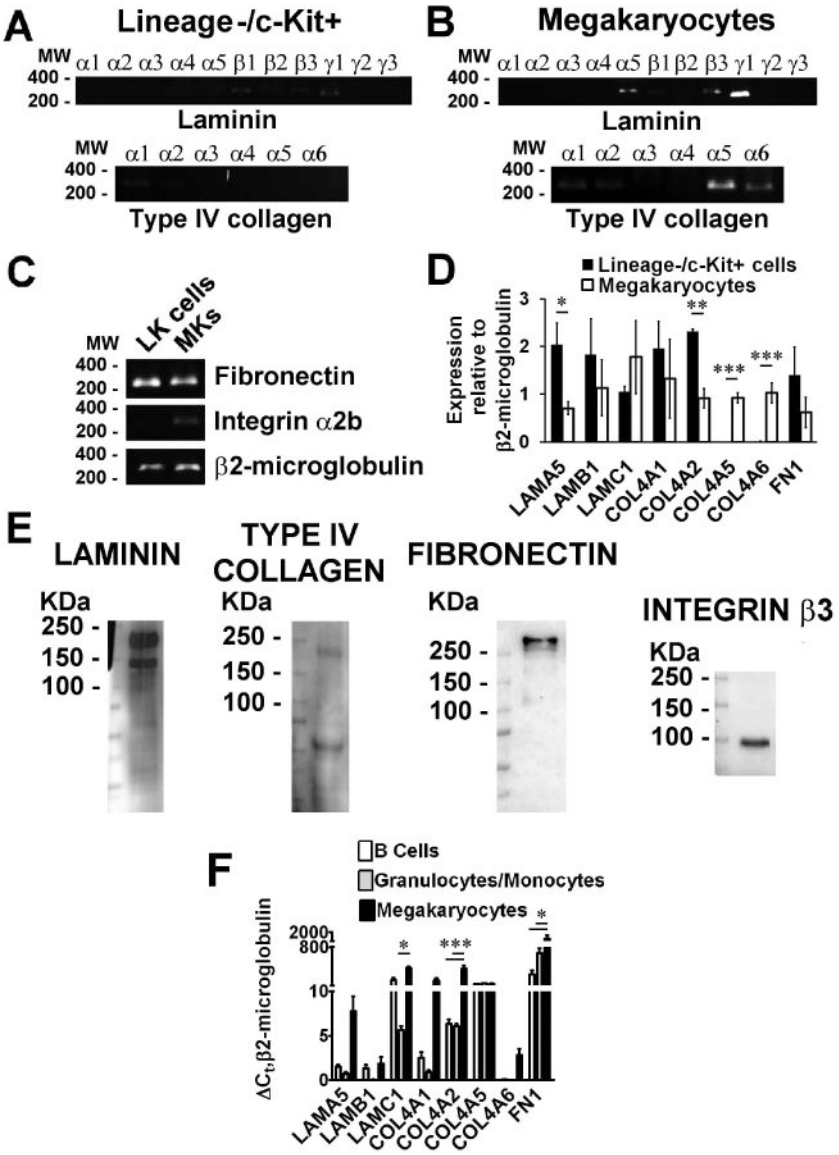

Figure 3.

Analysis of ECMs expression in bone marrow progenitors and mature Mks. RT-PCR was used to analyze the expression of mouse laminin and type IV collagen chains in **A**) Lineage negative/c-Kit+ (LK) bone marrow cells purified by immuno-magnetic separation and **B**) CD41+ cells purified by immuno-magnetic separation after 4 days of TPO driven differentiation. **C**) RT-PCR analysis of fibronectin, ITGA2b (Mk marker) and β2-microglobulin in both cell populations. **D**) qRT-PCR of ECM components expression during Mk development from lineage-/c-Kit+ cells enriched in hematopoietic progenitor cells. Data were normalized to β2-microglobulin expression in both cell populations. *p value=<0.05, **p value=0.01, ***p value=0.001. **E**) SDS-Page and western blotting analysis of laminin, type IV collagen and fibronectin in lysate of Mks derived from bone marrow progenitor cells. Integrin β3 (CD61) antibody was used to demonstrate Mk differentiation. **F**) ΔC_t, relative to β2-microglobulin, of ECMs expression in B220+ B Cells, Mac-1+ granulocytic/

monocytic cells and Mks sorted from bone marrow mononuclear cells in three independent samples. *p value=<0.05, ***p value=0.001.

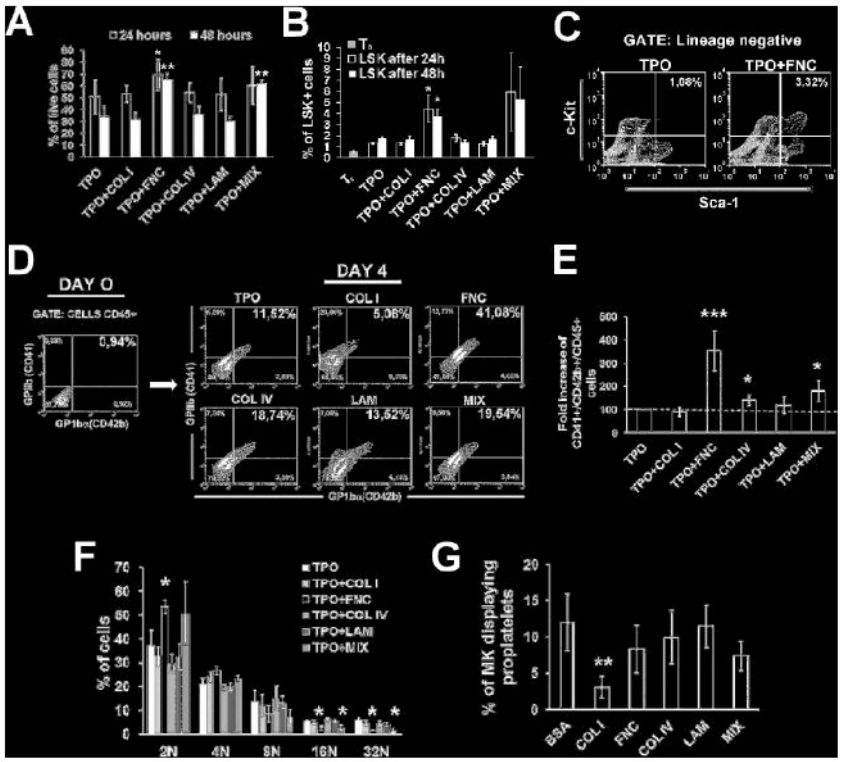

Figure 4.

In vitro effects of ECMs on HSC development and Mk differentiation. **A**) Flow cytometry analysis of 7-AAD viability measurements in lineage negative bone marrow cells after 24 and 48 hours of differentiation in the presence of TPO alone or combined with 10 μg of different ECMs. * p value=<0.05, **p value=0.01. **B**) LSK (Lineage-/Sca1+/c-Kit+) fraction in TPO or TPO plus ECMs treated cells after 24 and 48 hours of culture. T_0 represents the starting percentage of LSK in the purified lineage negative cell population, before TPO stimulation. p value=<0.05. **C**) Representative flow cytometry analysis of fibronectin (FNC) effect on the proliferation of LSK cells after 24 hours of culture with respect to cells treated with TPO alone. Cells were stained with FITC anti mouse lineage cocktail and LSK were identified with c-Kit-PE and Sca-1 APC antibodies in the lineage negative fraction. **D**) Lineage negative cells were selected from bone marrow cells by immunomagnetic beads and analyzed for their content in CD41+/CD42b+ cells in the CD45+ fraction, before cell culture (Day 0). Expression of Mk markers CD41 and CD42 were evaluated by flow cytometry in cells cultured for 4 days in the presence of TPO alone or TPO with 10 μg of different ECMs. **E**) Quantification of Mk number fold increase induced by different ECMs. p value *< 0.05, ***<0.001. **F**) Analysis of ECM effects on Mk ploidy after 4 days of culture as evaluated by flow cytometry after propidium iodide staining. **G)** Analysis of proplatelets formation after 24 hours of Mk adhesion on glass coverslips coated with different ECMs or BSA as control. p value **<0.01.

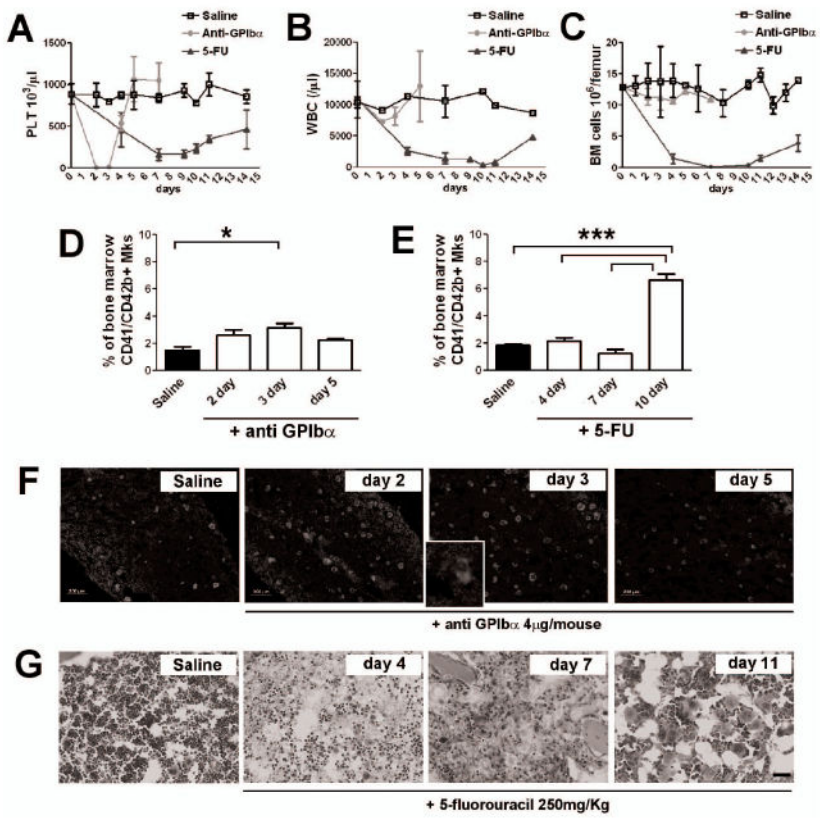

Figure 5.

In vivo analysis of Mk development after induced thrombocytopenia and during the recovery from 5-FU dependent myelosuppression. **A**) Peripheral platelet count in 5-FU and anti GPIbα treated mice. Blood samples from mice injected with PBS (Saline) were used as control. **B**) Peripheral leukocyte count during induced thrombocytopenia and myelosuppression in anti GPIbα and 5-FU treated mice. Only a slight decrease in white blood cells number was detected in peripheral blood of anti GPIbα treated mice, while blood cells reach their nadir around day 7 in mice injected with 5-FU to revert slowly to normal at day 14. **C**) Bone marrow mononuclear cells were counted in thrombocytopenic induced mice and 5-FU treated mice at different days of treatment. A complete leucopenia characterized femurs of 5-FU treated mice at day 4 and 7, while recovery started at day 11. At least three independent analysis were performed for each data point. **D-E**) Flow cytometry analysis of Mk content within bone marrow. Bone marrow cells of femurs from mice treated with PBS, as control, anti GPIbα (D) and 5-FU (E) were flushed and stained for Mk marker CD41 and CD42b. *p value < 0.05, ***p value < 0.001. **F**) Immunofluorescence analysis of Mk content in mice treated with anti GPIbα and PBS as control. CD41 (green) was used to highlight the increase in Mk number at day 2 and 3 of treatment before their return to normal level at day 5. Hoechst 33258 was used to stain nuclei (blue). Inset shows particular of the increase shedding of platelets within bone marrow at day 3 upon treatment. Images were acquired with a 10x objective. Scale bar=200μm. **G**) Hematoxylin & eosin staining of bone marrow section in control and 5-FU treated mice. In a week, a profound hypocellularity, vasculature regression and hemorrhages characterized the marrow

environment. By day 11 signs of recovery were demonstrated by the increase of marrow cells and by the expansion of the megakaryocytic lineage. 20x Objective. Scale bar=100μm.

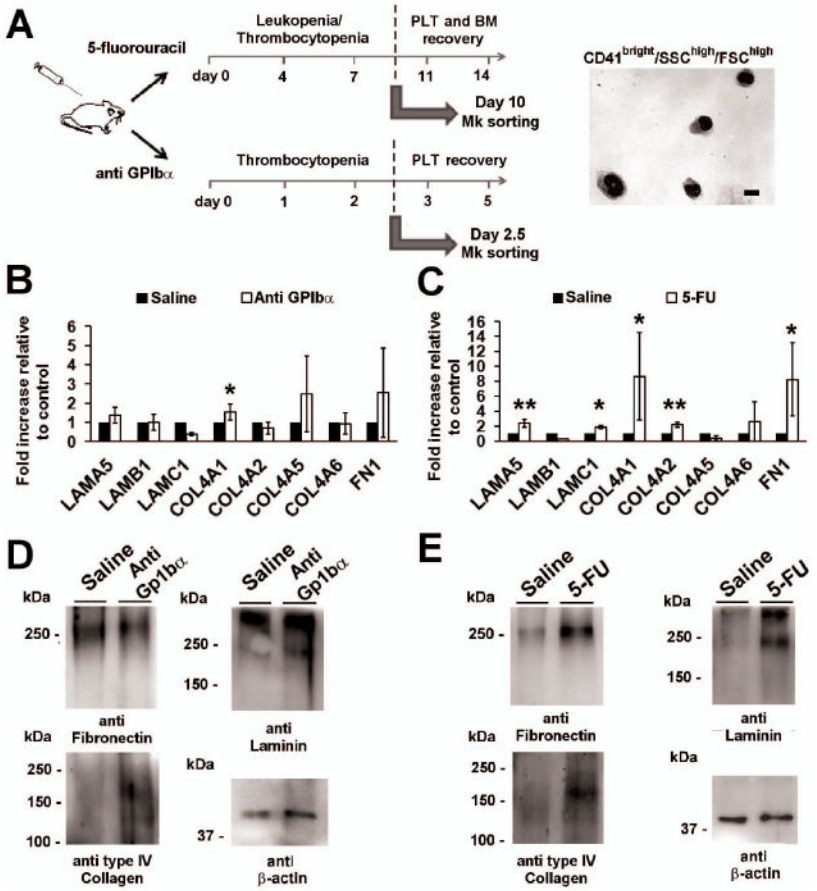

Figure 6.

Recovery of bone marrow niche after myelosuppression triggers the increase of ECM component synthesis by Mks *in vivo*. **A**) Schematic representation of the strategy adopted for Mk sorting in platelets depleted mice and 5-FU treated mice. Mk in mice injected with 4μg of anti GPIbα were sorted between at day 2.5 of treatment and just before the recovery of blood peripheral platelet count. In 5-FU treated mice, Mk were sorted at day 10 of treatment in juxtaposition of bone marrow and pheripheral blood count recovery. Right panel shows a representative hematoxylin & eosin staining of sorted Mks. Scale bar = 10 μm. **B**) RT-PCR of laminin, type IV collagen chains and fibronectin in Mks treated with PBS (Saline) or anti GPIbα. *p value < 0.05. **C**) RT-PCR of laminin, type IV collagen chains and fibronectin in Mks treated with PBS (Saline) or 5-FU. *p value 0.05, **p value 0.01. **D**) Western blotting analysis of ECM components level in Mks sorted from bone marrow cells after 60 hours of anti GPIbα antibody injection and PBS as control. **E**) Western blotting analysis of ECM components level in Mks sorted from bone marrow cells of mice myelosuppressed with 5-fluorouracil or PBS as control. β-Actin was revealed to demonstrate equal protein loading. The images are representative of three independent experiments.